Materiales de Construcción
Vol. 65, Issue 317, January–March 2015, e046
ISSN-L: 0465-2746
http://dx.doi.org/10.3989/mc.2015.00814

Synthesis of geopolymer from spent FCC: Effect of SiO_2/Al_2O_3 and Na_2O/SiO_2 molar ratios

J.J. Trochez[a], R. Mejía de Gutiérrez[a]✉, J. Rivera[a], S.A. Bernal[b]

a. Universidad del Valle, (Cali, Colombia)
b. University of Sheffield, (Sheffield, United Kingdom)
✉ruby.mejia@correounivalle.edu.co

Received 25 January 2014
Accepted 8 July 2014
Available on line 2 February 2015

ABSTRACT: This paper assesses the feasibility of using a spent fluid catalytic cracking catalyst (SFCC) as precursor for the production of geopolymers. The mechanical and structural characterization of alkali-activated SFCC binders formulated with different overall (activator + solid precursor) SiO_2/Al_2O_3 and Na_2O/SiO_2 molar ratios are reported. Formation of an aluminosilicate 'geopolymer' gel is observed under all conditions of activation used, along with formation of zeolites. Increased SiO_2/Al_2O_3 induces the formation of geopolymers with reduced mechanical strength, for all the Na_2O/SiO_2 ratios assessed, which is associated with excess silicate species supplied by the activator. This is least significant at increased alkalinity conditions (higher Na_2O/SiO_2 ratios), as larger extents of reaction of the spent catalyst are achieved. SiO_2/Al_2O_3 and Na_2O/SiO_2 ratios of 2.4 and 0.25, respectively, promote the highest compressive strength (67 MPa). This study elucidates the great potential of using SFCC as precursor to produce sustainable ceramic-like materials via alkali-activation.

KEYWORDS: Spent fluid catalytic cracking catalyst; Alkali-activation; Geopolymers; Structural characterization

Citation/Citar como: Trochez, J.J.; Mejía de Gutiérrez, R.; Rivera, J.; Bernal, S.A. (2015) Synthesis of geopolymer from spent FCC: Effect of SiO_2/Al_2O_3 and Na_2O/SiO_2 molar ratios. *Mater. Construcc.* 65 [317], e046 http://dx.doi.org/10.3989/mc.2015.00814.

RESUMEN: *Sintesis de geopolimero basado en un catalizador gastado de craqueo catalitico (FCC): Efecto de las relaciones molares SiO_2/Al_2O_3 y Na_2O/SiO_2.* Este artículo estudia la factibilidad de usar un catalizador gastado del proceso de craqueo (SFCC) para la producción de geopolímeros. Se evalúan las características mecánicas y estructurales de los geopolímeros producidos con diferentes relaciones molares (activador + precursor solido) de SiO_2/Al_2O_3 y Na_2O/SiO_2. La formación de un gel geopolimérico de tipo aluminosilicato se observa a las diferentes condiciones evaluadas, así como la formación de zeolitas. Un incremento en la relación SiO_2/Al_2O_3 genera geopolímeros de baja resistencia mecánica, a las diferentes relaciones molares Na_2O/SiO_2 evaluadas, como consecuencia del exceso de especies silicato provenientes del activador. Este efecto es menos significativo al incrementar las condiciones de alcalinidad (mayores relaciones Na_2O/SiO_2), ya que un mayor grado de reacción del catalizador gastado es alcanzado. Las relaciones SiO_2/Al_2O_3 y Na_2O/SiO_2 de 2.4 and 0.25, respectivamente, promueven la mayor Resistencia a la compresión (67 MPa). Este estudio muestra el gran potencial de uso del SFCC como precursor en materiales cerámicos obtenidos por activación alcalina.

PALABRAS CLAVE: Catalizador gastado de craqueo catalítico; Activación alcalina; Geopolimeros; Caracterización estructural

1. INTRODUCTION

The catalyst used in fluid catalytic cracking (FCC) in the petrochemical industry is an aluminosilicate with a zeolitic structure, often on an alumina or silica-alumina support. The FCC process is conducted to obtain higher-octane gasoline through the breaking of the long chains of hydrocarbon molecules. When the FCC catalyst loses its catalytic properties (becoming 'spent'), it is replaced, and the deactivated catalyst residue is discarded and treated as an inert waste (1).

In the search for ways to utilize this waste, the application of SFCC as an alternative supplementary cementitious material for the production of blended cements has been explored (2, 3). The pozzolanic activity of SFCC from different sources has been demonstrated, and the production of high performance Portland cement–based mortars and concretes has been achieved (1). Despite these evident good results, the availability of this by-product worldwide is relatively low, at around 800000 tons per year (4), and therefore, it has not been considered a commercially attractive alternative as a supplementary cementitious material in the global context. In Colombia, there is an estimated production 12400 tons/year of spent FCC, which is currently disposed in landfill. However, considering that SFCC can contain heavy metals, cementation of this waste is a viable alternative for its stabilization, rather than landfilling, which is the current disposal route in most parts of the world.

In the past decades great attention has been given to alternative cementitious materials known as 'geopolymers', which are binders produced through the chemical reaction between an aluminosilicate precursor and an alkaline activator. The main precursors used in geopolymers production are metakaolin (5) and industrial by-products from coal fired power generation, particularly fly ash (6–9). However, it has been proven that geopolymers can be produced from other aluminosilicate precursors, such as volcanic ashes (10, 11) and natural minerals (12, 13), whose composition is rich in silica and alumina present in energetic (usually disordered) solid phases. These precursors are easily dissolved in an alkaline media, promoting the subsequent polycondensation of the Al and Si species to form a hardened product (5).

The widespread interest in geopolymers for different industrial applications has motivated the assessment of low cost precursors such as SFCC in geopolymer production. Preliminary work activating SFCC catalysts to form geopolymers (14, 15) showed good mechanical strength in the activated SFCC specimens. This was attributed to the dissolution of the zeolite phases in the spent catalyst, promoting the formation of a crosslinked aluminosilicate type gel (15). The high reactivity of SFCC, along with its chemical composition rich in Al and Si, makes it a suitable precursor for production of geopolymers; however, there is not yet a good understanding of the mechanism of reaction of these materials, or detailed identification of the factors controlling their microstructural evolution. Also, it is expected that SFCC catalysts from different sources will have different compositions and structures, making necessary the assessment of different formulation conditions for each source of materials, to produce binders with good performance and to generate useful information by comparison of the performance of residues from different sources worldwide.

This study evaluates the feasibility of producing geopolymer materials based on a Colombian SFCC. The effect of formulation conditions, specifically overall Na_2O/SiO_2 and SiO_2/Al_2O_3 molar ratios, in the microstructure and compressive strength of these materials is assessed. Detailed structural analysis of the activated SFCC catalyst is conducted using X-ray diffraction (XRD), Fourier transform infrared spectroscopy (FTIR), ^{29}Si and ^{27}Al MAS nuclear magnetic resonance spectroscopy, and scanning electron microscopy (SEM).

2. EXPERIMENTAL PROGRAM

2.1. Materials

A spent fluid catalytic cracking catalyst (SFCC) from a Colombian petroleum company is used as the geopolymer precursor in this study. Before chemical activation, the SFCC was milled for 5 hours, using a ball mill. The resulting powder had specific gravity of 2630 kg/m^3 and a mean diameter D (4, 3) of 16.8 μm. The particle size distribution, determined by laser diffraction using a Mastersizer 200 of Malvern, was: 10% below 2.46 μm (D10), 50% below 13.25 μm (D50) and 90% below 37.44 μm (D90). Its chemical composition, determined by X-Ray Fluorescence (XRF) using a Philips MagixPro PW–2440 spectrometer fitted with a rhodium tube, is shown in Table 1.

TABLE 1. Chemical composition of the SFCC. LOI is loss on ignition at 1000 °C

Component	mass %
SiO_2	48.09
Al_2O_3	41.57
Fe_2O_3	0.91
CaO	0.22
MgO	0.13
K_2O	0.09
TiO_2	0.85
LOI	2.19

The X-ray diffractogram of the SFCC (Fig. 1) shows that this material contains an amorphous component, as well as the crystalline zeolite phases faujasite ($Na_2Al_2Si_{10}O_{24}{\cdot}nH_2O$, Powder Diffraction File (PDF) # 012-0228) and analcime ($NaAl_2Si_2O_6{\cdot}H_2O$, PDF # 003-0740), along with the aluminosilicate minerals andalusite (Al_2SiO_5, PDF # 039-0376), mullite ($2Al_2O_3{\cdot}SiO_2$, PDF # 089-2645), sillimanite ($Al_2O_3.SiO_2$, PDF # 089-0888), kyanite (Al_2SiO_5, PDF #00-011-046) and quartz (SiO_2, PDF # 046-1045).

The alkali activator used was a commercial sodium silicate solution with 29.1 wt.% SiO_2 and 10.2 wt.% Na_2O and 60.0 wt.% H_2O, and solid analytical grade NaOH pellets. This was dissolved in the mix water and allowed to cool until reaching room temperature prior to preparation of the specimens. All the activating solutions reach a pH higher than 14.

2.2. Sample preparation and tests conducted

For the preparation of the geopolymer specimens, the alkaline activator was formulated to obtain overall (activator + solid precursor) SiO_2/Al_2O_3 molar ratios of 2.0, 2.2, 2.4, 2.6, 2.8 and 3.0, and overall Na_2O/SiO_2 molar ratios of 0.20, 0.25 and 0.30. The amount of water in the alkali activator was adjusted to achieve a total H_2O/Na_2O ratio of 11 in all samples (Table 2). The fresh pastes were mixed for 12 minutes using a Hobart mixer, poured into cylindrical molds, and vibrated for 5 minutes to reach a homogeneous distribution in the mold and remove entrained air. Samples were kept in sealed molds at ambient temperature (25±5 °C) for 24 hours, then demolded and stored in a high humidity container (relative humidity >90%), also at ambient temperature, for 7 days.

The compressive strength was assessed for cylindrical paste samples of 30 mm (diameter) × 60 mm (height), using a universal testing instrument (Instron) at a displacement rate of 1 mm/min. Sample ends were flattened and made parallel using coarse sandpaper before testing. Each reported value corresponds to the average of 5 measurements. Powdered pastes were analyzed through:

- X-ray diffraction (XRD), using a Bruker D8 Advance instrument with Cu Kα radiation and a nickel filter. The tests were conducted with a step size of 0.020°, for 2θ values between 3° and 60°.
- Fourier transform infrared (FTIR) spectroscopy, with a PerkinElmer Spectrum 100 instrument. The KBr pellet technique was used to prepare the samples, which were scanned from 4000 to 400 cm^{-1}.
- Solid-state ^{29}Si and ^{27}Al magic angle spinning nuclear magnetic resonance (MAS NMR). The analysis of the SFCC was carried out with a Bruker 400 Ultrashield Avance II 400 spectrometer (9.4 T) using a MAS NMR probe for 5 mm rotors and a spinning speed of 5.0 kHz. ^{29}Si MAS NMR spectra were acquired using a resonance frequency of 79.5 MHz, a pulse width of 5 µs and a relaxation delay of 5 s and 4000 scans. ^{27}Al MAS NMR experiments were conducted at 104.23 MHz, with a pulse width of 5 µs, a relaxation delay of 0.25 s, and 2048 scans. MAS NMR spectra of the alkali activated specimens were obtained on a Varian Direct Drive VNMRS-600 spectrometer (14.1 T) using a MAS NMR probe for 4 mm o.d. zirconia rotors

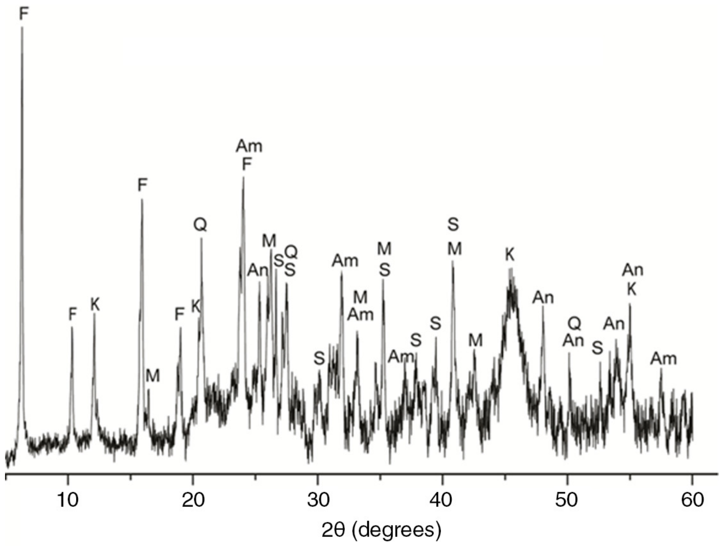

Figure 1. Diffractogram of the unreacted spent FCC catalyst. An: andalusite, Am: analcime, F: faujasite, K: kyanite, M: mullite, Q: quartz, S: sillimanite.

TABLE 2. Chemical Composition of geopolymer systems (total H_2O/Na_2O molar ratio of 11)

Mix Composition (Total Molar Ratio)			Alkaline activator Solution
SiO_2/Al_2O_3	Na_2O/SiO_2	Na_2O/Al_2O_3	$Ms=SiO_2/Na_2O$ (molar ratio)
2.0	0.20	0.40	0.08
2.2		0.44	0.53
2.4		0.48	0.90
2.6		0.52	1.22
2.8		0.56	1.49
3.0		0.60	1.72
2.0	0.25	0.50	0.07
2.2		0.55	0.42
2.4		0.60	0.72
2.6		0.65	0.97
2.8		0.70	1.19
3.0		0.75	1.38
2.0	0.30	0.60	0.06
2.2		0.66	0.35
2.4		0.72	0.60
2.6		0.78	0.81
2.8		0.84	0.99
3.0		0.90	1.15

and a spinning speed of 10.0 kHz. ^{29}Si MAS NMR spectra were acquired using a pulse width of 4 μs and a relaxation delay of 20 s, and more than 3600 scans. ^{27}Al MAS NMR experiments were conducted at 156.3 MHz on the same instrument, with a pulse width of 0.5 μs, a relaxation delay of 2 s, and 1024 scans. All ^{29}Si and ^{27}Al chemical shifts are referenced to external samples of tetramethylsilane (TMS) and a 1.0 M aqueous solution of $AlCl_3{\cdot}6H_2O$, respectively.

- Scanning electron microscopy (SEM), conducted in a JEOL JSM-6490LV high vacuum microscope ($3{\times}10^{-6}$ torr) at an acceleration voltage of 20 keV, using carbon coated unpolished specimens.

3. RESULTS AND DISCUSSION

3.1. Compressive strength

The formulation of the specimens has a marked effect on strength. The highest mechanical strengths are obtained (Fig. 2) in samples formulated with a Na_2O/SiO_2 ratio of 0.25 and a SiO_2/Al_2O_3 ratio of 2.4, reporting values of up to 67 MPa. In activated SFCC pastes formulated with a low Na_2O/SiO_2 ratio (0.20), a significant decrease in the mechanical strength is identified at higher SiO_2/Al_2O_3 ratios beyond the optimum. This effect is least pronounced at higher Na_2O/SiO_2 ratio (0.30), where activated spent catalyst samples formulated with SiO_2/Al_2O_3 ratios between 2.4 and 3.0 do not show significant changes in the compressive strength as a function of the formulation conditions. Specimens formulated with a Na_2O/SiO_2 molar ratio of 0.20 and SiO_2/Al_2O_3 of 2.0 and 2.2 were not tested due to the low degree of compaction achieved in these specimens.

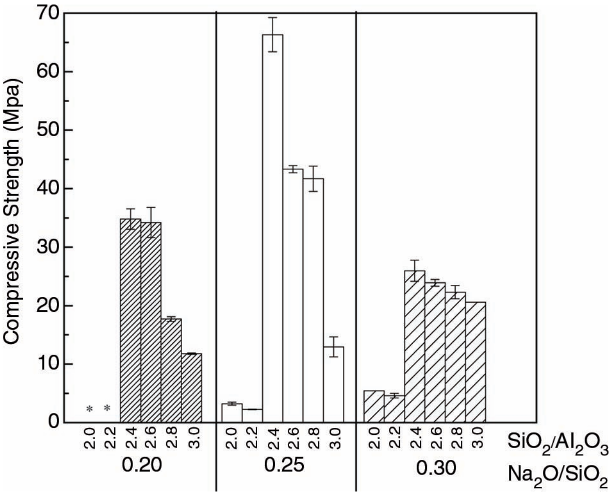

FIGURE 2. 7-day compressive strengths of alkali-activated SFCC specimens.

These results are comparable with the strengths of metakaolin-based geopolymers with the same curing duration and similar formulation conditions, including the reduction in strength at high SiO_2/Al_2O_3 ratios (16). This strength reduction is associated with the excess of silicates in the system supplied by the activator, as the extent of polymerization of the silica is high and its rate of reaction is slower than is required for optimal strength development (17). However, in the formulations with higher Na_2O/SiO_2 ratios, it is expected that the increased alkalinity promote a higher extent of dissolution of the spent catalysts, and therefore higher availability of Al-rich species, which are able to react with the additional silicate species that the activator can supply at higher SiO_2/Al_2O_3 ratios.

3.2. X-ray diffraction

The X-ray diffractograms of the activated spent FCC pastes formulated with Na_2O/SiO_2 molar ratios of 0.20, 0.25 and 0.30 are shown in Fig. 3. All of the activated SFCC pastes show (Figs. 3A, 3B and 3C) an amorphous hump

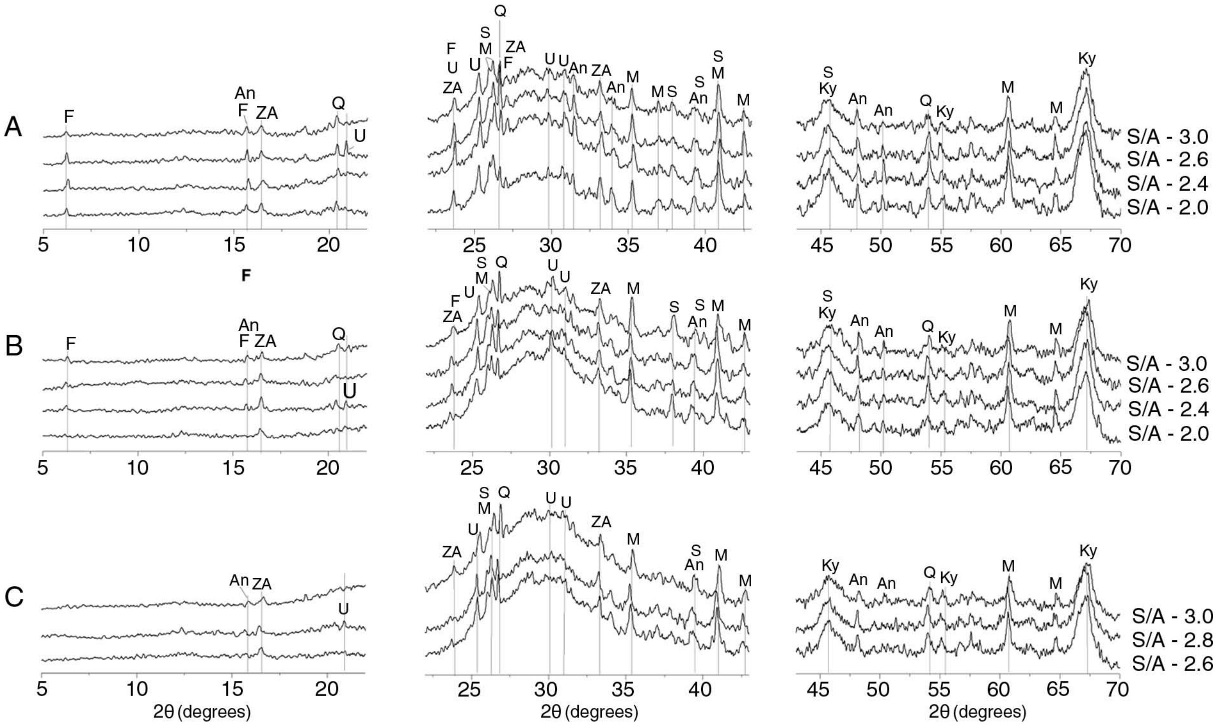

FIGURE 3. Diffractograms of activated SFCC pastes formulated with a Na_2O/SiO_2 ratio of (A) 0.20, (B) 0.25 and (C) 0.30. An: analcime, F: faujasite, U: ussingite, ZA: zeolite Na-A, Q: quartz, M: mullite, S: sillimanite and Ky: kyanite.

between 2θ values of 25° and 35°, attributed to the formation of an aluminosilicate type gel similar to those typically observed in metakaolin-based geopolymers (18). Mullite, sillimanite, kyanite and quartz, previously identified in the unreacted SFCC (Fig. 1), are also observed in the alkali-activated pastes, suggesting that these phases are not participating in the activation reaction to any notable extent. This is consistent with the observations in fly ash based geopolymers, where mullite and quartz are also identified as unreactive compounds (19), and the results of Rodríguez et al. (15) in alkali-activated specimens based on a Spanish SFCC material.

In samples formulated with an Na_2O/SiO_2 ratio of 0.20 (Fig. 3A), the intensities of the peaks assigned to faujasite and analcime are significantly reduced upon activation, when compared with the unreacted SFCC, along with the formation of zeolite Na-A ($Na_{12}Al_{12}Si_{12}O_{48}\cdot xH_2O$, PDF # 039-0221), which has been identified as a reaction product in geopolymer materials based on metakaolin (20). The formation of multiple zeolite phases embedded in the geopolymer gel has been reported in several studies (18), and our findings are consistent with these results. The formation of ussingite ($Na_2AlSi_3O_8(OH)$, PDF # 028-1037), which is a higher-silica secondary mineral often formed along with sodalite, is also observed under the activation conditions assessed.

Upon increasing the Na_2O/SiO_2 molar ratio to 0.25 (Fig. 3B), ussingite and zeolite Na-A are identified at the different SiO_2/Al_2O_3 ratios assessed. The intensity of the peaks assigned to faujasite is reduced upon activation. A similar trend is observed in the XRD patterns for the specimens formulated with the highest Na_2O/SiO_2 ratio (0.30) (Fig. 3C), where faujasite reflections are no longer observed. Considering this, and the fact that these samples have a more intense amorphous hump than specimens formulated with lower Na_2O/SiO_2 ratios, it is likely that faujasite is acting as a source of Al and Si species in the system, promoting the formation of an amorphous aluminosilicate type product. The excess hydroxide ion concentration, associated with higher Na_2O/SiO_2 ratios, is likely to influence the aluminosilicate gel precipitation at very early stages of reaction (21), promoting increased solubility, which affects the precipitation and the subsequent geopolymerization reactions. This is according with the results of compressive strength development presented in section 3.1.

3.3. Fourier transform infrared spectroscopy (FTIR)

The spectrum of unreacted SFCC (Fig. 4) shows bands at 912 cm^{-1} corresponding to the OH deformation vibration (22), and the signals at 834, 612 and 526 cm^{-1} attributed to asymmetric, double 6-ring, and bending vibration modes of the aluminosilicate

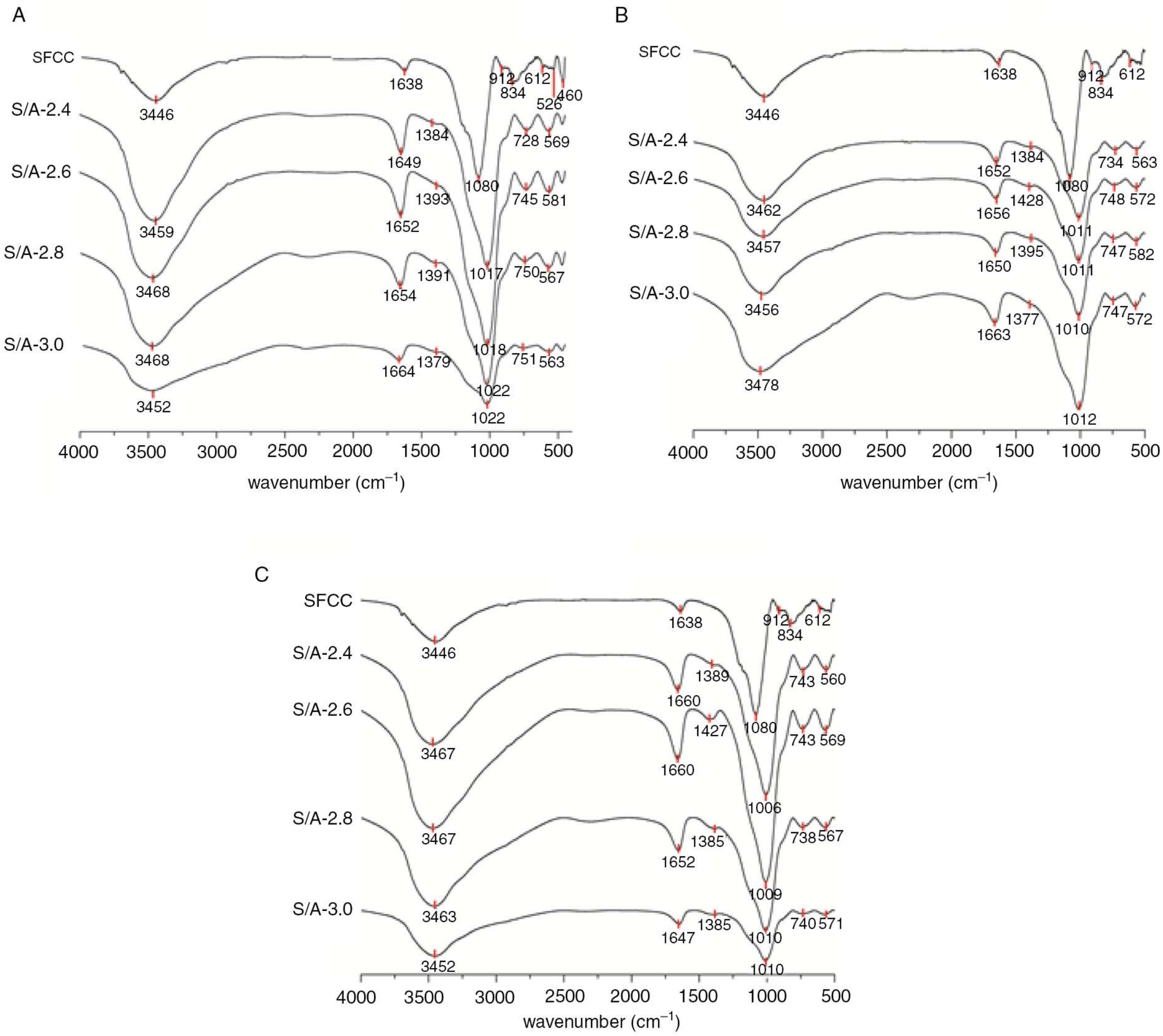

FIGURE 4. FTIR spectra of SFCC precursor, and activated pastes formulated with SiO_2/Al_2O_3 (S/A) ratios as marked, at Na_2O/SiO_2 ratios of (A) 0.20, (B) 0.25, (C) 0.30.

framework in dealuminated faujasite (23). The band at 560 cm^{-1} is assigned to the octahedral aluminum present in mullite, kyanite and sillimanite, as identified by XRD (Fig. 1), and the band at 460 cm^{-1} corresponds to the symmetric bending modes of the Si-O-Si bonds (24).

All alkali-activated pastes display a main band between 1200 cm^{-1} and 800 cm^{-1} corresponding to the asymmetric stretching vibration mode of the Si-O-T linkage (where T may be Si or Al) (25). It is observed that this band shifts towards lower wavenumbers (~1011 cm^{-1}) upon activation of the anhydrous SFCC precursor (1080 cm^{-1}). This displacement suggests a structural change of the SFCC upon partial dissolution in the alkaline environment, and the subsequent formation of an aluminosilicate type gel.

The activation process also leads to a reduction in the intensities of the bands observed in the SFCC precursor at 460 cm^{-1}, 526 cm^{-1} and 617 cm^{-1}, associated with the dissolution of the zeolite phases, consistent with the XRD results (Fig. 3). It is likely that the highly alkaline environment promotes the dissolution of the SFCC initially through the breaking of Al-O bonds, considering that this type of bonds has a lower energy (~60 kcal/mol) than Si-O bonds (~80 kcal/mol) (26).

Bands at 1630 cm^{-1} and 3450 cm^{-1} in the activated pastes are attributed to bending (H–O–H) and stretching vibrations (–OH) of water in the hydrated products, respectively (27). The higher intensity of these bands in the alkali activated pastes, compared with the SFCC precursor, is consistent with more adsorbed water groups ($\equiv Si-OH \ldots H_2O$ and $\equiv Al-OH \ldots H_2O$) in the aluminosilicate gel (28).

In samples with an Na_2O/SiO_2 molar ratio of 0.20, a lower SiO_2/Al_2O_3 ratio promotes shifting of the

T-O-T band towards lower wavenumbers (1017 cm^{-1} for SiO_2/Al_2O_3=2.4), suggesting the incorporation of higher contents of Al within the gel, compared with the samples activated with higher SiO_2/Al_2O_3 ratio that show slight variations in the T-O-T band position (1022 cm^{-1} for SiO_2/Al_2O_3=3.0). These results are consistent with the formation of a more Si-rich gel in the samples formulated with the highest SiO_2/Al_2O_3 ratio. This is in agreement with the shifting of the band at 725 cm^{-1} towards higher wavenumbers at increased SiO_2/Al_2O_3 ratios, as a consequence of the more Si-rich environment in the gel. The Si-O-T band is observed to be narrower and significantly more intense for the samples with SiO_2/Al_2O_3 ratios of 2.4 and 2.6, because of the higher extent of dissolution of the SFCC, contributing more silicate and aluminate species for geopolymer gel formation. Similar trends are observed in specimens formulated with higher Na_2O/SiO_2 ratios (0.25 and 0.30).

At higher alkalinity conditions, associated with higher Na_2O/SiO_2 ratios, the alkali content favors the initial dissolution of the aluminosilicate precursor and its consequent reaction to form the geopolymer product. This leads to the shifting of the main T-O-T band towards lower wavenumbers as identified in the activated specimens when compared with the unreacted SFCC. Conversely, at low alkalinity conditions a higher proportion of unreacted precursor is identified, as the T-O-T band of the SFCC does not exhibit variations in the activated samples.

3.4. ^{29}Si and ^{27}Al MAS NMR spectroscopy

Figure 5 shows the ^{27}Al MAS spectrum of the unreacted SFCC, with broad bands in the regions assigned to octahedrally (Al(VI)) (−10 to 30 ppm), tetrahedrally (Al(IV)) (50 to 80 ppm), and minor pentahedrally (Al(V)) (30 to 50 ppm) coordinated Al environments. The intense peak in the 10 ppm region is mainly attributed to the octahedral aluminum species present in kyanite and sillimanite phases (29), and extra-framework Al(VI) species in the dealuminated zeolites identified through XRD (Fig. 1). The resonance near 60 ppm is assigned to the tetrahedrally coordinated Al in the zeolites present in the SFCC (30). The intensity at 45 ppm is ascribed to a less ordered framework where Al atoms are present in imperfectly crystalline zeolites. The FCC catalyst suffers hydrothermal dealumination through its use in the catalytic cracking process where up to 90% of the tetrahedrally-coordinated Al in the zeolite framework is removed, and consequently the bonds involving Al are replaced by hydroxyl groups linked to silicon (31).

The ^{29}Si MAS spectrum of the unreacted SFCC (Fig. 6) shows a dominant resonance near −105 ppm, attributed to the Q^4(0Al) sites of the highly dealuminated faujasite resulting from the different stages in the cracker unit (32), and also a contribution from quartz (−107 ppm) as identified via XRD (Fig. 1). The asymmetry of this band suggests that it overlaps with a wide range of resonances from different Si-containing phases identified in the SFCC, and therefore cannot be attributed to a single phase.

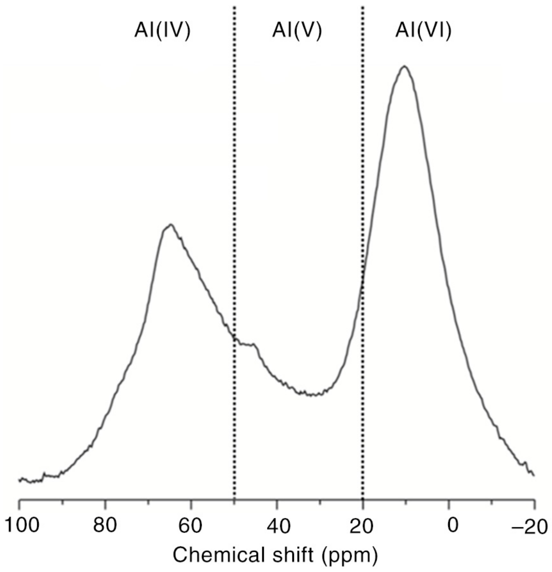

FIGURE 5. ^{27}Al MAS NMR spectrum of the unreacted SFCC.

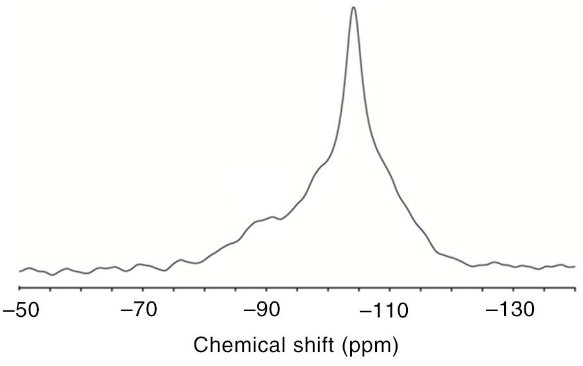

FIGURE 6. ^{29}Si MAS NMR spectrum of the unreacted SFCC.

The ^{27}Al MAS spectra of selected SFCC-based geopolymers (Fig. 7) show changes in the line shape compared with unreacted SFCC (Fig. 5). The Al(V) resonance observed between 30 and 50 ppm (Fig. 7) in the unreacted precursor completely disappears upon activation, consistent with the high reactivity of Al(V) sites. In alkali activation of aluminosilicates, it has been shown that Al(V) and Al(VI) are converted to tetrahedral sites (Al(IV)) with an associated alkali cation to maintain electroneutrality (33).

A significant reduction of the Al(VI) band is identified in the activated SFCC, when compared with the unreacted SFCC, along with a significant

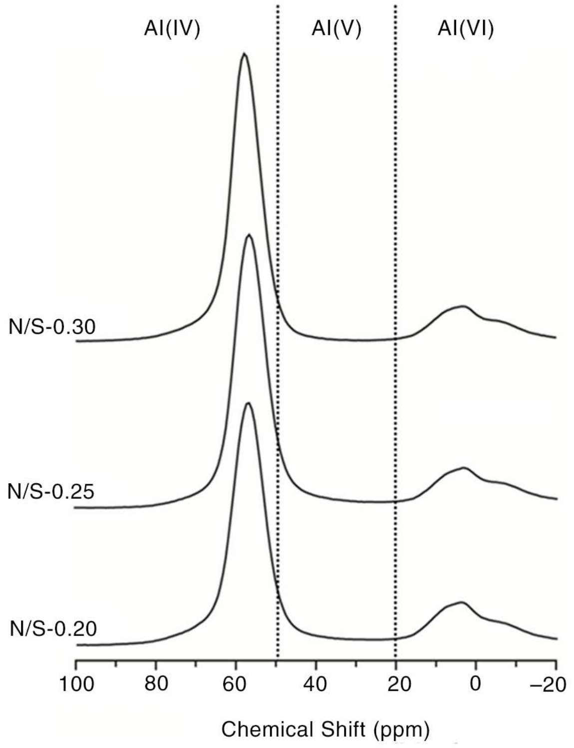

FIGURE 7. ^{27}Al MAS NMR spectra of SFCC geopolymers formulated with a SiO_2/Al_2O_3 ratio of 2.4, as a function of Na_2O/SiO_2 (N/S) ratio as marked.

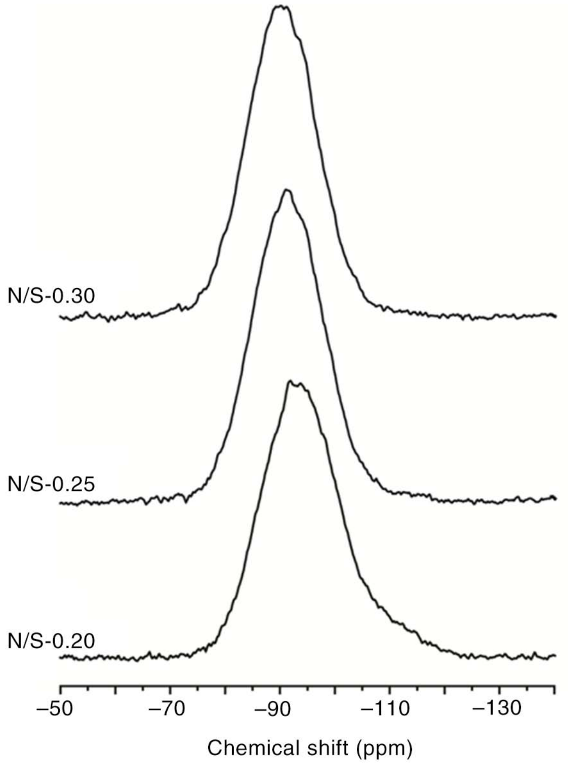

FIGURE 8. ^{29}Si MAS NMR spectra of SFCC geopolymers formulated with a SiO_2/Al_2O_3 ratio of 2.4, as function of the Na_2O/SiO_2 (N/S) ratio.

increase in the intensity in the Al(IV) region of the spectra. The reduction in the intensity of the bands in the Al(VI) region is attributed to the dissolution of the dealuminated zeolite, leading to the formation of a highly crosslinked disordered aluminosilicate 'geopolymer' gel, as identified by FTIR.

Although the ^{27}Al MAS NMR spectra of the activated SFCC specimens are dominated by the resonance associated with Al(IV), a small resonance centered between 2 and 3 ppm is also observed in the spectra. This resonance corresponds to small amounts of Al(VI) from the residual mullite phase (34), identified in the XRD after the activation (Fig. 3). The amount of Al(IV) increases as the alkali content (Na_2O/SiO_2 ratio) increases from 0.20 to 0.30, in good agreement with the formation of a larger amount of aluminosilicate type gel, as observed via FTIR, and in good agreement with the decrease in intensity of the Al(VI) band remaining from unreacted material.

The peak at −105 ppm in the ^{29}Si MAS NMR spectrum of the unreacted SFCC (Fig. 8) is no longer identified in the geopolymer specimens, consistent with the dissolution of faujasite upon activation as observed via XRD (Fig. 3). The ^{29}Si MAS NMR spectra of the alkali activated SFCC binders (Fig. 8) show a broad band centered at −91 ppm assigned to Q^4(3Al) sites, consistent with the incorporation of Al in the geopolymer gel. The spectrum of activated SFCC is within the region assigned to Q^4(4Al), Q^4(3Al), Q^4(2Al) and Q^4(1Al) sites, overlapping with the sites in the residual unreacted precursor, which means that it is difficult to identify particular sites from the unreacted spent catalyst and the newly forming phases.

Low alkali content (Na_2O/SiO_2 of 0.20) promotes the broadening of the ^{29}Si MAS NMR spectrum, along with a low intensity shoulder between −98 ppm and −120 ppm, corresponding to the Q^4 sites of faujasite from the spent catalyst that are not completely consumed during the geopolymerisation process. Increasing the alkali content (higher Na_2O/SiO_2), the intensity of this shoulder is significantly reduced, confirming a higher extent of dissolution of faujasite from the SFCC at higher alkali content in the systems, as observed in the XRD results (Fig. 3). The main band also becomes slightly narrowed and more intense when the Na_2O/SiO_2 ratio is increased from 0.20 to 0.30, indicating a higher degree of ordering of the gel formed, in good agreement with the ^{27}Al NMR results (Fig. 7).

3.5. Scanning electron microscopy

Figure 9 shows evident differences in the density, surface smoothness, and proportion of unreacted particles in activated SFCC as a function of

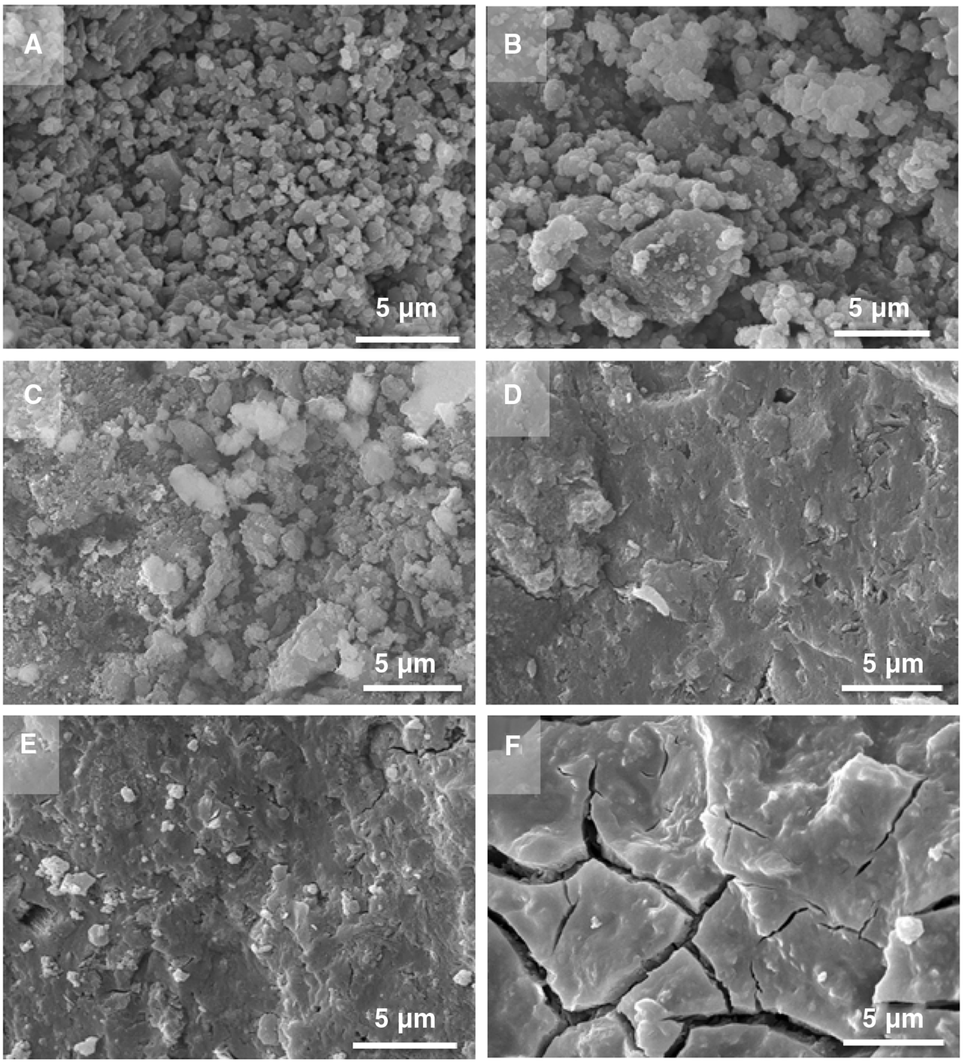

FIGURE 9. SEM images of geopolymers formulated with an Na_2O/SiO_2 molar ratio of 0.25, and SiO_2/Al_2O_3 molar ratios of (A) 2.0 (B) 2.2 (C) 2.4 (D) 2.6, (E) 2.8 and (F) 3.0.

formulation conditions, as a more homogeneous and dense microstructure is identified in specimens with increased SiO_2/Al_2O_3 ratio. The visibly low densities exhibited by samples formulated with SiO_2/Al_2O_3 of 2.0 and 2.2 are consistent with their low compressive strengths (Fig. 2), this can be associated with a low degree of reaction of the SFCC under these activation conditions. Although the highest mechanical strength is obtained in samples formulated with a SiO_2/Al_2O_3 ratio of 2.4, its microstructure (Fig. 9C) is not as dense as in specimens formulated with a SiO_2/Al_2O_3 ratio of 2.6 (Fig. 9D). This suggests that the materials might be more brittle at these activation conditions. Samples formulated with an SiO_2/Al_2O_3 ratio greater than 2.6 (Figs. 9E, F) show large cracks associated with severe shrinkage, which can lead to the reduced mechanical strength observed at these activation conditions.

4. CONCLUSIONS

Geopolymers can be successfully produced from spent fluid catalytic cracking catalyst, which is available in high volumes in some parts of the world. Structural studies show that the alkali-activated SFCC pastes consist of an amorphous phase corresponding to an aluminosilicate ‘geopolymer’ type gel, along with different types of zeolites, depending on the contents of silicates and alkalis available in the systems. The mechanical strength of the activated SFCC is strongly influenced by the formulation conditions, where optimal overall SiO_2/Al_2O_3 and Na_2O/SiO_2 ratios of 2.4 and 0.25, respectively, promoting a compressive strength of up to 67 MPa. Insufficient alkali content in the formulated geopolymers retards the initial dissolution of the zeolite phases present in the SFCC, and consequently a higher proportion of unreacted precursor is identified in the samples activated with an Na_2O/SiO_2 molar ratio of 0.20. These results elucidate that alkali-activation of SFCC is a viable method for managing and valorizing this industrial waste, with great potential for the production of ceramic-like materials with good mechanical performance.

ACKNOWLEDGMENTS

This study was sponsored by the *Universidad del Valle* (Colombia), the Center of Excellence of Novel Materials (CENM) and *Colciencias*. The authors would like to thank Drs. John Gehman and Rackel San Nicolas (U. Melbourne) for NMR data acquisition, and Prof. John L. Provis (U. Sheffield) for valuable discussions.

REFERENCES

1. Zornoza-Gómez, E. (2007) El papel del catalizador usado de craqueo catalítico (fcc) como material puzolánico en el proceso de corrosión de armaduras de hormigón, in Departamento de Ingeniería de la Construcción y de Proyectos de Ingeniería Civil. Universitat Politécnica de Valencia: Valencia- España. 328.
2. Pacewska, B.; Wilińska, I.; Kubissa, J. (1998) Use of spent catalyst from catalytic cracking in fluidized bed as a new concrete additive. *Thermochim. Acta* 322 [2], 175–181. http://dx.doi.org/10.1016/S0040-6031(98)00498-5.
3. Payá, J.; Monzó, J.; Borrachero, M.V. (1999) Fluid catalytic cracking catalyst residue (FC3R): An excellent mineral by-product for improving early-strength development of cement mixtures. *Cem. Concr. Res*. 29 [11],1773–1779. http://dx.doi.org/10.1016/S0008-8846(99)00164-7.
4. Letzsch, W. (2010) Global demand for catalytic technology increases. Available from: http://www.hartfuel.com/f.catalyst.html.
5. Duxson, P.; Fernández-Jiménez, A.; Provis, J.L.; Lukey, G.C.; Palomo, A.; van Deventer, J.S.J. (2007) Geopolymer technology: The current state of the art. *J. Mater. Sci*. 42 [9], 2917–2933. http://dx.doi.org/10.1007/s10853-006-0637-z.
6. Duxson, P.; Provis, J.L. (2008) Designing precursors for geopolymer cements. *J. Am. Ceram. Soc*. 91 [12], 3864–3869. http://dx.doi.org/10.1111/j.1551-2916.2008.02787.x.
7. Puertas, F.; Martínez-Ramírez, S.; Alonso, S.; Vázquez, T. (2000) Alkali-activated fly ash/slag cements: Strength behaviour and hydration products. *Cem. Concr. Res*. 30 [10], 1625–1632. http://dx.doi.org/10.1016/S0008-8846(00)00298-2.
8. Kovalchuk, G.; Fernández-Jiménez, A.; Palomo, A. (2008) Alkali-activated fly ash. Relationship between mechanical strength gains and initial ash chemistry. *Mater. Construcc*. 58 [291], 35–52. http://dx.doi.org/10.3989/mc.2008.v58.i291.
9. Mejía, J.M.; Mejía de Gutiérrez, R.; Puertas, F. (2013) Rice husk ash as a source of silica in alkali-activated fly ash and granulated blast furnace slag systems. *Mater. Construcc*. 63 [311], 361–375. http://dx.doi.org/10.3989/mc.2013.04712.
10. Shi, C.; Day, R.L. (1993) Chemical activation of blended cements made with lime and natural pozzolans. *Cem. Concr. Res*. 23 [6], 1389–1396. http://dx.doi.org/10.1016/0008-8846(93)90076-L.
11. Najafi Kani, E.; Allahverdi, A.; Provis, J.L. (2012) Efflorescence control in geopolymer binders based on natural pozzolan. *Cem. Concr. Compos*. 34 [1], 25–33. http://dx.doi.org/10.1016/j.cemconcomp.2011.07.007.
12. Xu, H.; van Deventer, J.S.J. (2000) The geopolymerisation of alumino-silicate minerals. *Int. J. Miner. Proc*. 59 [3], 247–266. http://dx.doi.org/10.1016/S0301-7516(99)00074-5.
13. Feng, D.; Provis, J.L.; van Deventer, J.S.J. (2012) Thermal activation of albite for the synthesis of one-part mix geopolymers. *J. Am. Ceram. Soc*. 95 [5], 565–572. http://dx.doi.org/10.1111/j.1551-2916.2011.04925.x.
14. Tashima, M.M.; Akasaki, J.L.; Castaldelli, V.N.; Soriano, L.; Monzó, J.; Payá, J.; Borrachero, M.V. (2012) New geopolymeric binder based on fluid catalytic cracking catalyst residue (FCC). *Mater. Lett*. 80, 50–52. http://dx.doi.org/10.1016/j.matlet.2012.04.051.
15. Rodríguez, E.D.; Bernal, S.A.; Provis, J.L.; Gehman, J.D.; Monzó, J.M.; Payá, J.; Borrachero, M.V. (2013) Geopolymer based on spent catalyst residue from a fluid catalytic cracking (FCC) process. *Fuel*. 109, 493–502. http://dx.doi.org/10.1016/j.fuel.2013.02.053.
16. Bernal, S.A.; Rodríguez, E.D.; Mejía de Gutierrez, R.; Gordillo, M.; Provis, J.L. (2011) Mechanical and thermal characterisation of geopolymers based on silicate-activated metakaolin/slag blends. *J. Mater. Sci*. 46 [16], 5477–5486. http://dx.doi.org/10.1007/s10853-011-5490-z.
17. Duxson, P.; Provis, J.L.; Lukey, G.C.; Mallicoat, S.W.; Kriven, W.M.; van Deventer, J.S.J. (2005) Understanding the relationship between geopolymer composition, microstructure and mechanical properties. *Colloids Surfaces A* 269 [1–3], 47–58. http://dx.doi.org/10.1016/j.colsurfa.2005.06.060.
18. Provis, J.L.; Lukey, G.C.; van Deventer, J.S.J. (2005) Do geopolymers actually contain nanocrystalline zeolites? - A reexamination of existing results. *Chem. Mater*. 17 [12], 3075–3085. http://dx.doi.org/10.1021/cm050230i.
19. Lloyd, R.R.; Provis, J.L.; van Deventer, J.S.J. (2009) Microscopy and microanalysis of inorganic polymer cements. 1: Remnant fly ash particles. *J. Mater. Sci*. 44 [2], 608–619. http://dx.doi.org/10.1007/s10853-008-3077-0.
20. Gualtieri, A.; Norby, P.; Artioli, G.; Hanson, J. (1997) Kinetics of formation of zeolite Na-A [LTA] from natural kaolinites. *Phys. Chem. Miner*. 24 [3], 191–199. http://dx.doi.org/10.1007/s002690050032.
21. Somna, K.; Jaturapitakkul, C.; Kajitvichyanukul, P.; Chindaprasirt, P. (2011) NaOH-activated ground fly ash geopolymer cured at ambient temperature. *Fuel* 90 [6], 2118–2124. http://dx.doi.org/10.1016/j.fuel.2011.01.018.
22. Madejova, J.; Komadel, P. (2001) Baseline studies of the Clay Minerals Society source clays: Infrared methods. *Clays Clay Miner*. 49 [5], 410–432.
23. Miessner, H.; Kosslick, H.; Lohse, U.; Parlitz, B.; Tuan, V.A. (1993) Characterization of highly dealuminated faujasite-type zeolites: ultrastable zeolite Y and ZSM-20. *J. Phys. Chem*. 97, 9741–9748. http://dx.doi.org/10.1021/j100140a034.
24. Farmer V.C. The Infrared Spectra of Minerals. London: Mineralogical Society, 1974.
25. Rees, C.A.; Provis, J.L.; Lukey, G.C.; van Deventer, J.S.J. (2007) Attenuated total reflectance Fourier transform infrared analysis of fly ash geopolymer gel aging. *Langmuir* 23 [15], 8170–8179. http://dx.doi.org/10.1021/la700713g.
26. Provis, J.L.; Duxson, P.; Lukey, G.C.; van Deventer, J.S.J. (2005) Statistical thermodynamic model for Si/Al ordering in amorphous aluminosilicates. *Chem. Mater*. 17 [11], 2976–2986. http://dx.doi.org/10.1021/cm050219i.
27. Rees, C.A. Mechanisms and Kinetics of Gel Formation in Geopolymers, Ph.D. Thesis. University of Melbourne: Melbourne, Australia, 2007.
28. Zhang, Z.; Wang, H.; Provis, J.L.; Bullen, F.; Reid, A.; Zhu, Y. (2012) Quantitative kinetic and structural analysis of geopolymers. Part 1. The activation of metakaolin with sodium hydroxide. *Thermochim. Acta* 539, 23–33. http://dx.doi.org/10.1016/j.tca.2012.03.021.
29. Hartman, J.S.; Sherriff, B.L. (1991) Silicon-^{29} MAS NMR of the aluminosilicate mineral kyanite: residual dipolar coupling to aluminum-^{27} and nonexponential spin-lattice relaxation. *J. Phys. Chem*. 95 [20], 7575–7579. http://dx.doi.org/10.1021/j100173a005.
30. Occelli, M.L.; Voigt, U.; Eckert, H. (2004) The use of solid state nuclear magnetic resonance (NMR) to study the effect of composition on the properties of equilibrium fluid

cracking catalysts (FCCs). *Appl Catal. A* 259, 245–251. http://dx.doi.org/10.1016/j.apcata.2003.09.032.

31. Rakiewicz, E.F.; Mueller, K.T.; Jarvie, T.P.; Sutovich, K.J.; Roberie, T.G.; Peters, A.W. (1996) Solid-state NMR studies of silanol groups in mildly and highly dealuminated faujasites. *Microporous Mater*. 7, 81–88. http://dx.doi.org/10.1016/0927-6513(96)00031-4.
32. Behera, B.; Ray, S.S. (2009) Structural changes of FCC catalyst from fresh to regeneration stages and associated coke in a FCC refining unit: A multinuclear solid state NMR approach. *Catal. Today* 141 [1], 195–204. http://dx.doi.org/10.1016/j.cattod.2008.03.017.
33. Duxson, P.; Lukey, G.C.; Separovic, F.; van Deventer, J.S.J. (2005) The effect of alkali cations on aluminum incorporation in geopolymeric gels. *Ind. Eng. Chem. Res*. 44 [4], 832–839. http://dx.doi.org/10.1021/ie0494216.
34. Merwin, L.H.; Sebald, A.; Rager, H.; Schneider, H. (1991) ^{29}Si and ^{27}Al MAS NMR spectroscopy of mullite. *Phys. Chem. Miner*. 18, 47–52. http://dx.doi.org/10.1007/BF00199043.